Effects of Winds and Breaking Waves on Large-Scale Coastal Currents Developed by Winter Storms in Japan Sea

Shinji SATO
Dr. Eng., Senior Researcher, Coastal Eng. Division,
Public Works Research Institute

(Received Sep 17, 1996; Revised Nov. 1, 1996)

Coastal Engineering in Japan
Vol. 39, No. 2
December 1996
Japan Society of Civil Engineers

Coastal Engineering in Japan, Vol. 39, No. 2, 1996

EFFECTS OF WINDS AND BREAKING WAVES ON LARGE-SCALE COASTAL CURRENTS DEVELOPED BY WINTER STORMS IN JAPAN SEA*

Shinji Sato [1]

ABSTRACT

Field data obtained in the offshore region of two coasts facing the Japan Sea revealed that strong large-scale alongshore currents were generated and significant change in bed elevation was developed during winter storms. The currents were observed in a wide area extending from surf zone to offshore region. The development of the currents was simulated by a numerical model based on the depth-integrated momentum equation. The model included the effects of the wind drag at sea surface, the Coriolis force, the momentum transfer by surface wave breaking and the interaction with nearshore currents in surf zone. Effects of the large-scale currents on the evolution of coastal topography around large-scale structures were also discussed.

Keywords: coastal currents, wind-driven currents, wave breaking, evolution of coastal topography

I. INTRODUCTION

Severe storms are frequently generated in winter on the Japan Sea, which are caused by periodic passages of low-pressure systems across the sea. The winter storm generally persists for several days, generating strong winds and large waves from northwest. During the storm, strong alongshore currents are also observed in the offshore region, which may continue to flow over a couple of days. The estimation of the currents, which are almost as strong as nearshore currents in surf zone, is important since those currents will exert strong influence on various coastal processes, such as the propagation of wind waves and the sand transport during the storm.

In order to evaluate long-term large-scale coastal evolution, it is essential to understand sand transport mechanisms outside of the surf zone. Although sediment transport outside of surf zone is relatively weak compared with that in surf zone, various strong currents were observed near the bottom which may contribute to long-term evolution of the coastal topography (Niedroda and Swift, 1991). These currents are generated by the global wind system, the variation in the gravitational force due to the relative motion of the sun and the moon, and the difference in the sea water density. On the basis of the comparison of numerical experiments with field data, Sato (1995) showed that the strong alongshore currents observed near the bottom of

*A part of this study was orally presented at the 43rd Japanese Conference on Coastal Engineering, November 1996.

[1]Dr. Eng., Senior Researcher, Coastal Eng. Division, Public Works Research Institute

Niigata coast at the depth of 15m were identified as large-scale coastal boundary currents which were developed and maintained by the wind stress and the Coriolis force. However, since the comparison was made only with the data obtained at a single point, the scale of the currents and the interaction of the currents with wave-induced currents were not understood well.

The objective of this study is to investigate the dynamics of waves, currents and sand movement during winter storms. The mechanism of the generation of the strong currents in the offshore region is described on the basis of field data as well as numerical experiments. The effects of the offshore currents on the nearshore currents and the sediment movement will be described in detail.

II. ANALYSIS OF FIELD DATA

Field investigations were performed at Ishikawa and Niigata coasts facing the Japan Sea (see Fig. 1) during the period from December 1994 to February 1995. On both coasts, the beaches are covered with fine sand and the bottom topographies are of simple contour lines parallel to the shoreline with mean bed slope about 1/100. Three pairs of ultrasonic wave gages and current meters were installed on each coast.

2.1 Field Data Obtained at Ishikawa Coast

The left side of Fig. 2 shows arrangements of instruments used at Ishikawa coast. Two sets of wave gages and current meters were situated at the depths of 10.6 m and 15.1 m off Tokumitsu. Another set was installed at the depth of 15.1 m off Shimbori river-mouth, which was 30 km to the southwest of Tokumitsu, in order to confirm the alongshore scale of the currents in the offshore region. The elevation of the current meter was 0.6 m above the bottom. In addition to the measurements of waves and currents, the bed elevation at Tokumitsu 15.1 m was monitored by an optical bed elevation sensor which detected the bed elevation change by pairs of optical sensors fixed on 1 m rods with a spacing of 2.5 cm. The movement of sand at Tokumitsu 15.1 m was also investigated by fluorescent sand tracer test. The fluorescent sand was placed on December 23, 1994 and sampled on January 17, 1995, at eight points situated in a circular area with 2 m radius around the injection point. Small amount of fluorescent sand was found in all the samples except for one obtained at the south of the injection point, indicating significant sand movement at the site.

Temporal variations of data obtained at Tokumitsu 15.1 m were shown in Fig. 3. The upper part of Fig. 3 shows mean water level $\overline{\eta}$, atmospheric pressure η_p, the significant wave height $H_{1/3}$, the significant wave period $T_{1/3}$, current velocity u near the bottom, wind velocity W, which were evaluated from 20 min record obtained every hour. The atmospheric pressure p_0 was converted to the equivalent water level change η_p by $\eta_p = (\overline{p}_0 - p_0)/(\rho_w g)$, where ρ_w is the density of sea water, g the gravity acceleration and $\overline{p}_0$ the mean atmospheric pressure. A few storms were generated in the observation period by the passage of low-pressure system across the Japan Sea. The rise in the mean water level as well as the generation of strong waves and currents were observed during storms. The currents, which exceeded 40 cm/s on January 5 and 10, were mostly developed in the alongshore direction. Northeast ward currents were especially strong since strong winds from W to NW prevailed during storms. The strong alongshore currents were considered to be explained as coastal boundary

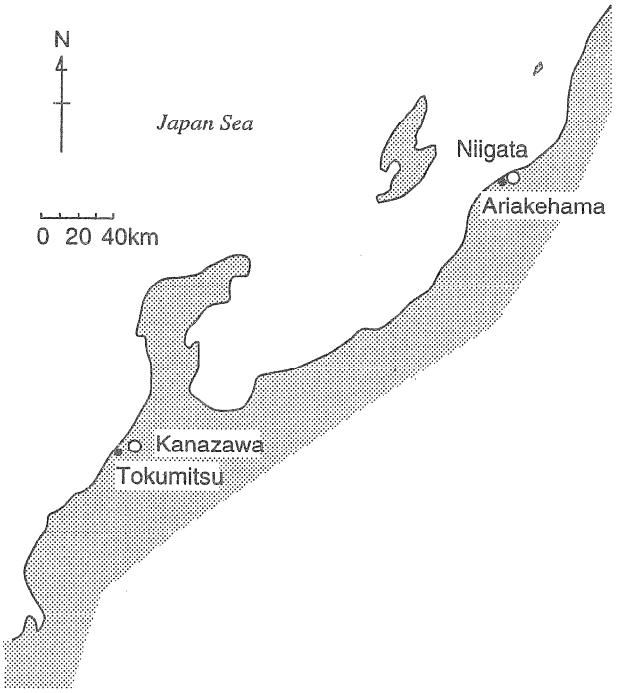

Fig. 1 Field observation sites.

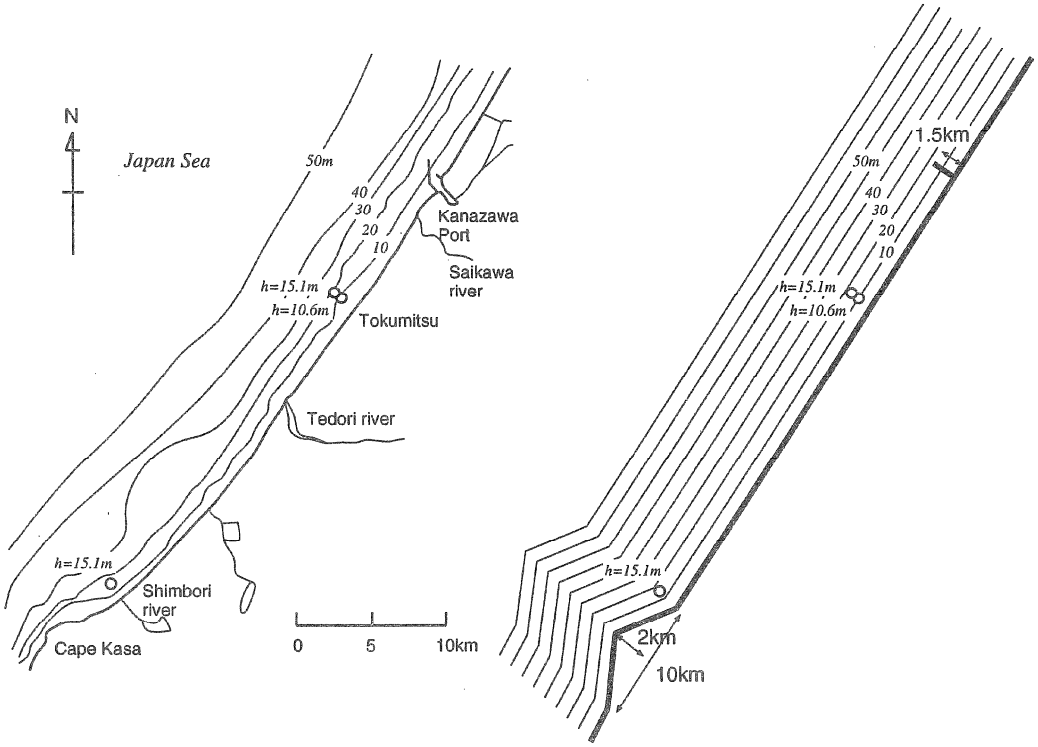

Fig. 2 Arrangement of instruments at Ishikawa coast (left) and modeled coastal topography used in the numerical model (right).

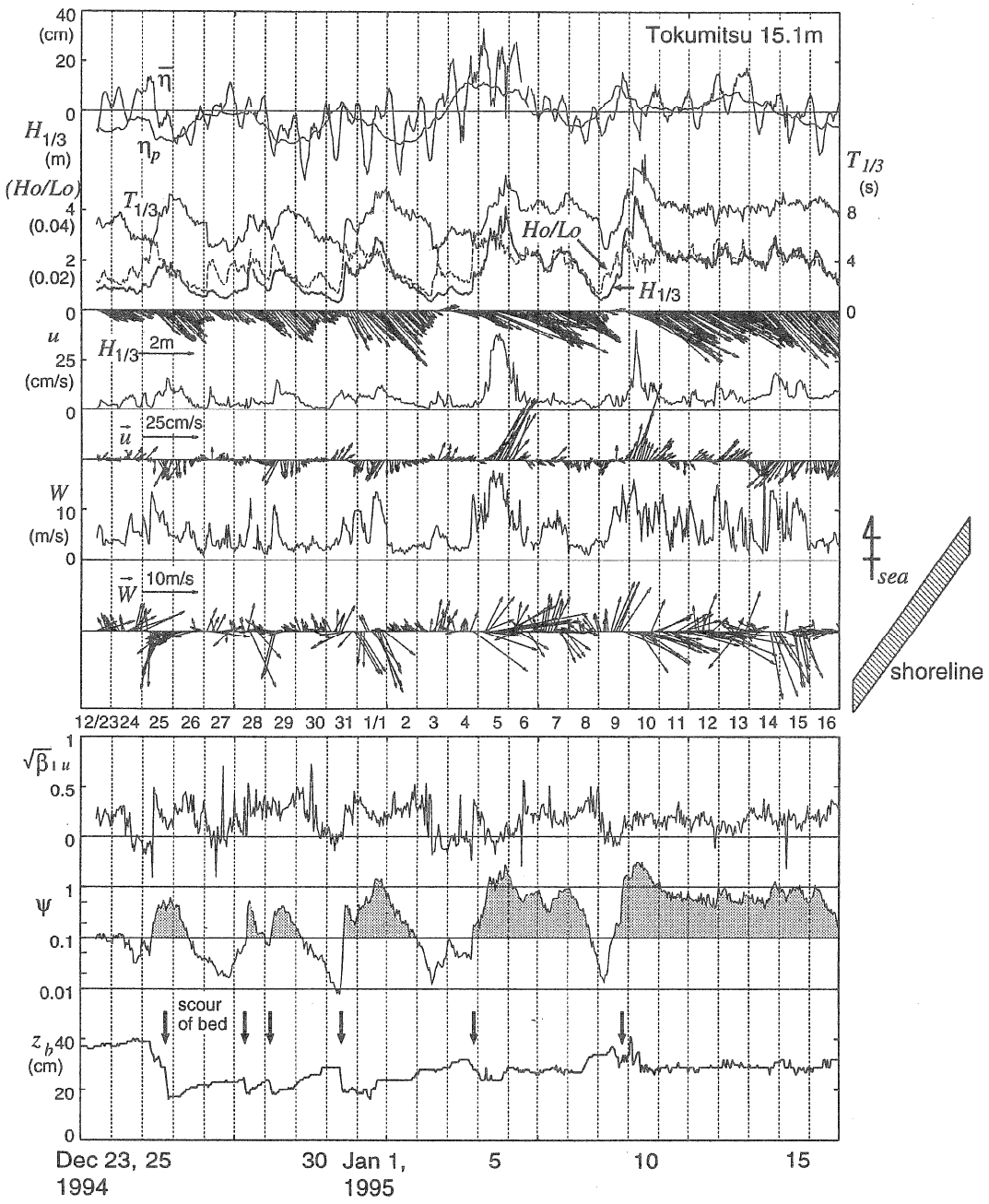

Fig. 3 Temporal variation of winds, waves, currents and bottom elevation at Ishikawa coast.

currents developed by the effects of the wind stress and the Coriolis force, as was explained in Sato (1995).

The lower part of Fig. 3 shows variations of the bed elevation z_b, the skewness

$\sqrt{\beta_1}_u$ in near-bottom velocity u_b and the Shields parameter Ψ defined as follows:

$$\sqrt{\beta_1}_u = \frac{\overline{(u_b - \bar{u}_b)^3}}{[\overline{(u_b - \bar{u}_b)^2}]^{3/2}} \tag{1}$$

$$\Psi = \frac{1}{2} f_w \frac{\hat{u}_b^2}{(\rho_s/\rho_w - 1)gD} \tag{2}$$

where f_w is the wave friction factor, $\hat{u}_b$ the velocity amplitude near the bottom estimated in terms of the significant wave height, ρ_s the density of sand particles and D the diameter of sand particles. The diameter of sand particles was estimated at $D = 0.15$ mm from sieve analysis of sand samples. The change in bed elevation was significant when the Shields parameter exceeded 0.1. It is also noticed however that significant change in bed elevation does not always occur under high waves, when the Shields parameter is on the order of unity. The bed elevation showed a sudden decrease at the early stage of storm when the velocity skewness $\sqrt{\beta_1}_u$ and the Shields parameter Ψ increased rapidly. Since the sudden scour of bed occurred only at the beginning of storms, it is difficult to explain it by local scour around the sensor. After the sudden scour of bed, the bed was recovered gradually in a couple of days. The sudden scour of the bed was considered to be due to the spatial imbalance in the shoreward transport of sediment in the offshore region. The spatial imbalance in the longshore transport was considered to be too small to generate a sudden change in bed elevation since the alongshore currents observed in the offshore was of large scale. On the assumption that the bed elevation was changed only by the imbalance in the cross-shore transport rate, the distribution of the cross-shore sand transport rates was estimated as shown in Fig. 4, where Q denotes the cross-shore sand transport rate and Δz_b the correspondent bed elevation change. The shoreward sediment transport enhanced in the offshore region was due to the asymmetric wave orbital motion under steep waves observed at the early stage of the storm whereas seaward transport dominated in surf zone was considered to be due to undertow. The steep gradient in Q in the offshore region was considered to be responsible for the sudden scour of the offshore bed. In the subsequent stages of a storm, gradual recovery of the offshore bed was expected by offshore-directed transport of suspended sediment.

Waves and currents observed at Tokumitsu 10.6 m and Shimbori 15.1 m are illustrated in Fig. 5. Compared with the current velocity at Tokumitsu 15.1 m (Fig. 3), currents at Tokumitsu 10.6 m are stronger especially when the wave height is large. This is considered to be due to the acceleration of the currents by the gradient of radiation stresses developed in surf zone. Currents at Shimbori 15.1 m are directed in the same direction as those at Tokumitsu but are weak in general, suggesting that the currents might be weakened by the sheltering effect of the Cape Kasa. The effect of coastal topography on current magnitude will be discussed later with a numerical experiment.

Sato (1995) showed on the basis of field data obtained at Niigata coast that strong northwestern wind during a winter storm caused a rise in sea water level near the shoreline as well as the generation of strong alongshore currents. Figure 6 shows the relationship between the alongshore component of the current velocity and that of the wind velocity for the data obtained at Tokumitsu. In order to identify the effect of

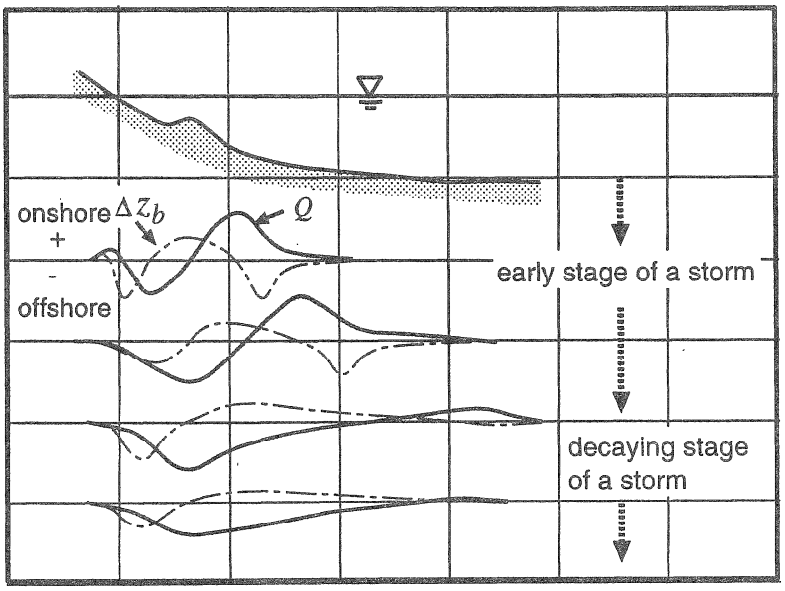

Fig. 4 Distribution of cross-shore sand transport rate and expected bed elevation change during a storm.

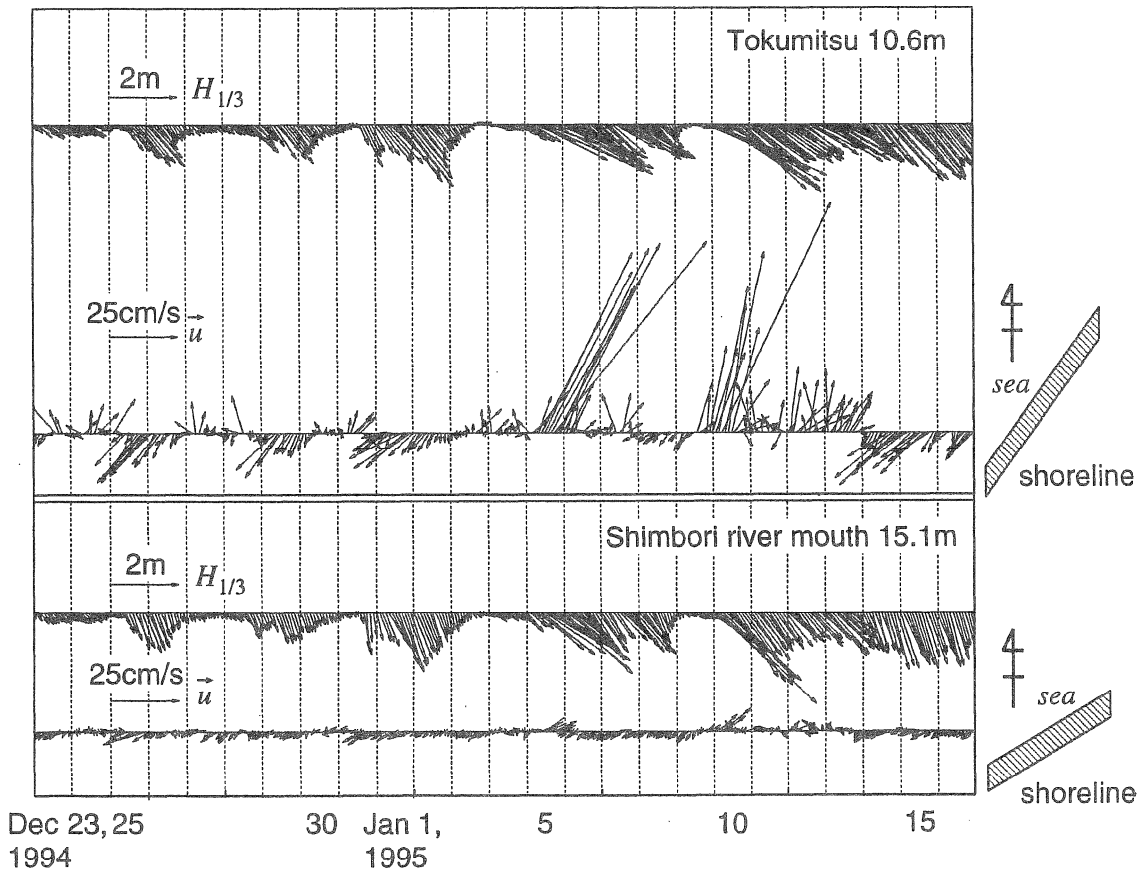

Fig. 5 Temporal variation of waves and currents at Ishikawa coast.

obliquely incident waves on the currents, the plot was classified in terms of H_s defined as follows:

$$H_s = H_{1/3} \frac{\vec{k} \cdot \vec{s}}{|\vec{k}|} \tag{3}$$

where $\vec{k}$ is the wavenumber vector and $\vec{s}$ the unit vector parallel to the shoreline. Longshore currents with $u_s > 0$ will be developed in surf zone when $H_s > 0$. It is confirmed in Fig. 6 that the magnitude of the current velocity increases as wind velocity increases. However, the current velocities at the depth of 10.6 m are sensitive to the wave height. This is because the currents at the depth of 10.6 m are accelerated by longshore currents developed in surf zone. It is also noted that the currents at the depth of 15.1 m are also accelerated under large waves, although it is less obvious than those at 10.6 m.

2.2 Field Data Obtained at Niigata Coast

On Niigata coast, the instruments were situated in the cross-shore direction at the depths of 20.0 m, 15.4 m and 8.8 m as shown in Fig. 7, aiming at the investigation of the interaction of offshore coastal currents induced by wind and nearshore longshore currents induced by wave breaking. Measurements were carried out from November 24, 1994 to March 1, 1995.

Figure 8 shows the data in the same period as those of Ishikawa coast. Strong northwestern winds were dominant during a storm in the same manner as Ishikawa coast. However, compared with Ishikawa coast where the incident angle of large waves varied in a broad range from W to NNW, storm waves on Niigata coast were incident from a narrow range around NNW. This is due to the presence of Sado Island in front of Niigata coast, which sheltered waves incident from the northwest (see Fig. 1). It is also confirmed in Fig. 8 that the strong alongshore currents during a storm prevailed in a wide area extending from the edge of the breaker zone to the offshore region where the water depth is of the order of 20 m. The width of the currents was more than 1 km.

III. LARGE-SCALE CURRENTS DEVELOPED BY WINDS AND WAVES

3.1 Numerical Model

Numerical experiments were performed in order to determine the essential physical mechanisms involved in the generation of the strong alongshore currents. The currents and the mean water level change induced by strong winds were numerically simulated on the basis of the following depth-integrated mass and momentum equations:

$$\frac{\partial \eta}{\partial t} + \frac{\partial Q_x}{\partial x} + \frac{\partial Q_y}{\partial y} = 0 \tag{4}$$

$$\begin{aligned} &\frac{\partial Q_x}{\partial t} + \frac{\partial}{\partial x}\left(\frac{Q_x^2}{d}\right) + \frac{\partial}{\partial y}\left(\frac{Q_x Q_y}{d}\right) - f Q_y + g d \frac{\partial \eta}{\partial x} + \frac{d}{\rho_w}\frac{\partial p_0}{\partial x} \\ &+ \frac{1}{\rho_w}\left(\frac{\partial S_{xx}}{\partial x} + \frac{\partial S_{xy}}{\partial y}\right) - \frac{\tau_{sx}}{\rho_w} + \frac{\tau_{bx}}{\rho_w} - \epsilon\left(\frac{\partial^2 Q_x}{\partial x^2} + \frac{\partial^2 Q_x}{\partial y^2}\right) = 0 \end{aligned} \tag{5}$$

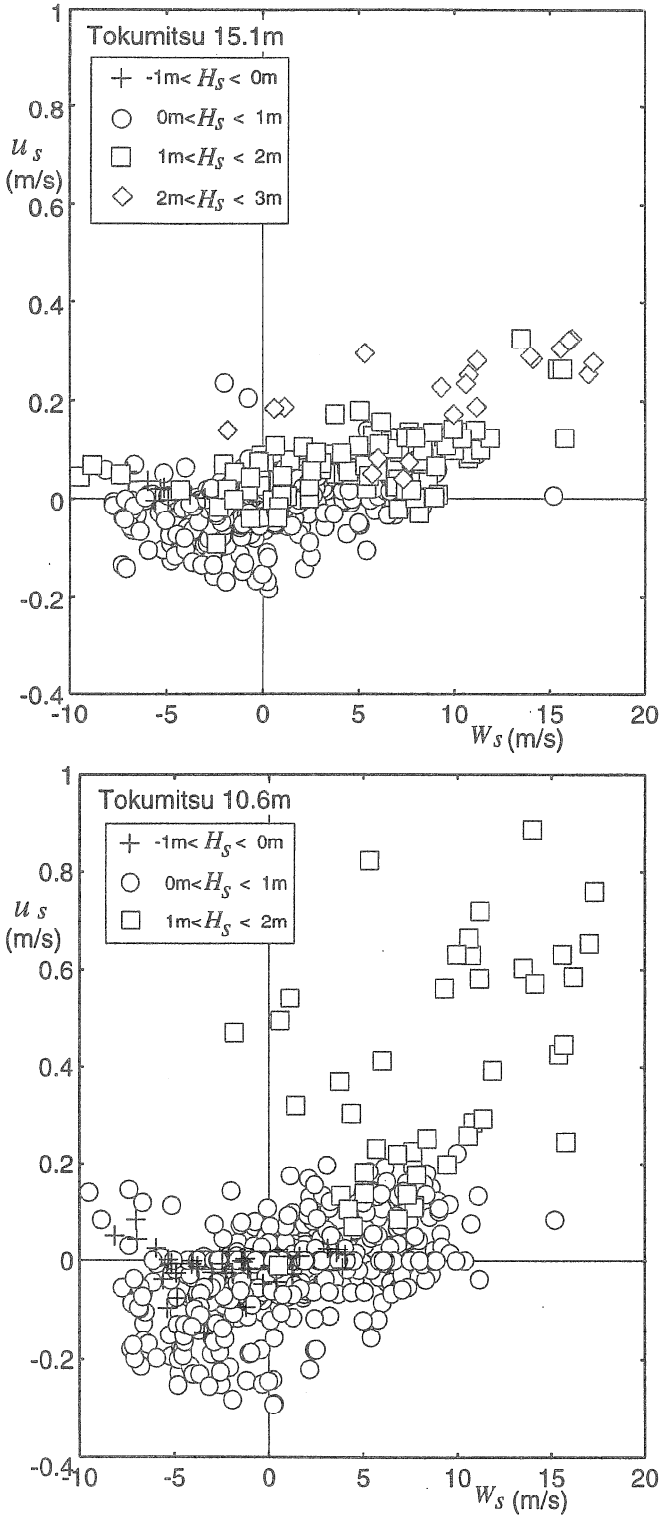

Fig. 6 Relationship between alongshore components of current velocity and wind velocity.

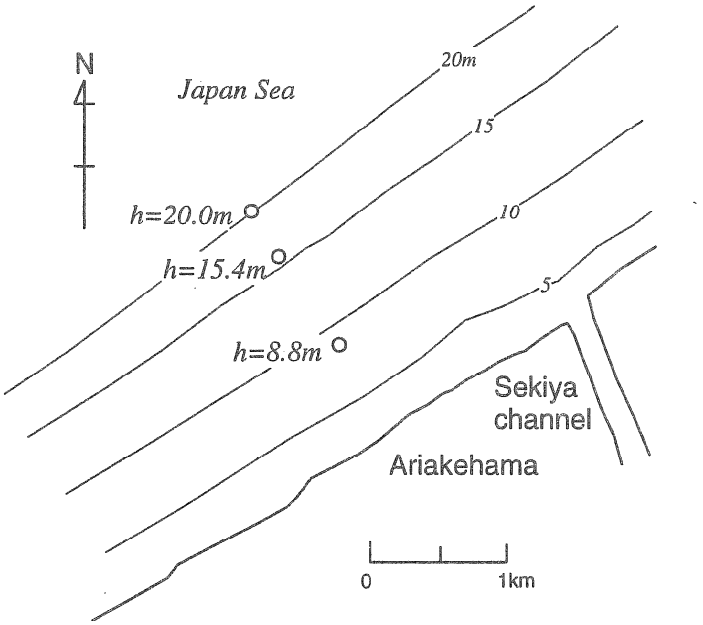

Fig. 7 Arrangement of instruments at Niigata coast.

$$\frac{\partial Q_y}{\partial t} + \frac{\partial}{\partial x}\left(\frac{Q_x Q_y}{d}\right) + \frac{\partial}{\partial y}\left(\frac{Q_y^2}{d}\right) + fQ_x + gd\frac{\partial \eta}{\partial y} + \frac{d}{\rho_w}\frac{\partial p_0}{\partial y}$$
$$+ \frac{1}{\rho_w}\left(\frac{\partial S_{yx}}{\partial x} + \frac{\partial S_{yy}}{\partial y}\right) - \frac{\tau_{sy}}{\rho_w} + \frac{\tau_{by}}{\rho_w} - \epsilon\left(\frac{\partial^2 Q_y}{\partial x^2} + \frac{\partial^2 Q_y}{\partial y^2}\right) = 0 \qquad (6)$$

where Q_x and Q_y are flow rates in the x and y directions respectively, η the surface elevation, $d(= h+\eta,\ h$ the still water depth) the total depth, τ_s and τ_b the wind stress and the bottom shear stress respectively, S_{xx}, S_{xy} and S_{yy} the radiation stresses, $f(= 2\omega \sin\phi$, where ω is the angular frequency of earth rotation and ϕ the latitude) the Coriolis coefficient and ϵ the horizontal eddy viscosity.

The computational domain was a rectangular area of 100 km in the alongshore direction and 30 km in the cross-shore direction. The sea bottom slope was set at 1/100 which was of the same order as the mean beach slope of Ishikawa and Niigata coasts. The governing equations were numerically integrated by an efficient ADI algorithm (Sato, 1995). The grid size was 200 m in an area within a distance of 3km from the shoreline and 1km elsewhere. The wind speed was assumed to be uniform in the entire domain. Temporal wind variations observed on the coast were used as the input to the model, which simulated the generation of large-scale currents in the offshore region as well as nearshore currents in surf zone.

The surface stress due to wind was estimated by,

$$\vec{\tau}_s = \rho_a C_a \vec{W}|\vec{W}| \qquad (7)$$

where ρ_a is the density of air and C_a is the drag coefficient of sea surface. The bottom

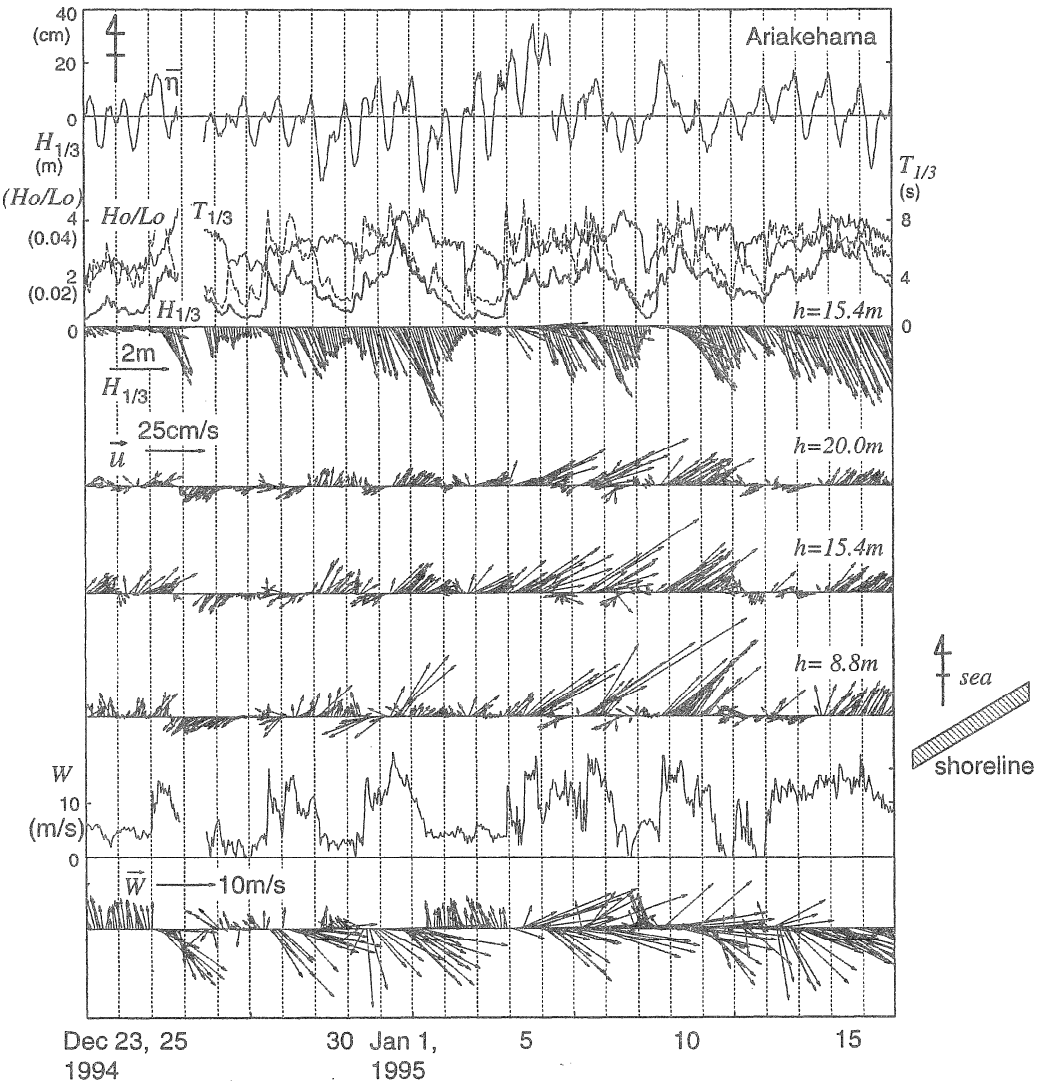

Fig. 8 Temporal variation of waves and currents at Niigata coast.

shear stress was modeled by Manning's formula,

$$\vec{\tau}_b = \frac{\rho_w g n^2}{d^{1/3}} \vec{u}|\vec{u}| \tag{8}$$

where n is a roughness parameter, which was determined at $n = 0.026$ ($\mathrm{m}^{1/3}\mathrm{s}$) typically used in storm surge simulation. On the basis of the data obtained at Tokumitsu in which the currents are regarded equilibrium where the surface drag due to wind balanced the bottom shear stress, the value of C_a was estimated to be $C_a = 0.001$. The value is consistent with the laboratory measurements of wind waves (Honda and Mitsuyasu, 1980).

The radiation stress was estimated from random wave shoaling model presented by Goda and Watanabe (1991) which showed that the cross-shore distribution of longshore currents could be simulated by considering wave randomness without using

unrealistic large value for the eddy viscosity ϵ. The offshore wave height distribution was determined as the Rayleigh distribution and the change in the wave height distribution was computed by using random wave breaking model of Goda (1975). The distribution of the radiation stress was then estimated from that of $H_{\rm rms}$.

Longuet-Higgins (1970) introduced the following formula for eddy viscosity,

$$\epsilon = N l_x \sqrt{gh} \tag{9}$$

where $N(< 0.016)$ is a non-dimensional coefficient and l_x is the distance from the shoreline. When the eddy viscosity is evaluated from Eq. (9) for a typical storm condition observed on Ishikawa and Niigata coasts, the eddy viscosity is evaluated at the order of 25 m^2/s for waves with significant wave height of 4 m breaking on a 1/100 sloping beach. In the present study, since the radiation stress was estimated with the effect of wave randomness, the simulated longshore currents would have a smooth profile even if the value of the eddy viscosity was set at zero (Goda and Watanabe, 1991). The value of the eddy viscosity was therefore set in the present model at a small value of 1 m^2/s which provided stable computation.

3.2 Effect of Waves

In surf zone, longshore currents will be developed by obliquely incident waves. Wind driven currents, on the other hand, will be generated in the direction of winds, so that the currents outside of surf zone and those in surf zone may be opposite when the wave direction and the wind direction are opposite with respect to the sea bottom contours. Figure 9 illustrates variations of waves, currents and winds observed at Niigata coast from January 30 to February 2, 1995. On January 31, all the currents at h = 8.8 m, 15.4 m and 20.0 m were directed to the northeast owing to strong winds from the west. However, after February 1 when waves from NNW increased their heights, the currents direction changed to southwest and west. The reversal of the currents started from surf zone and gradually extended to the offshore region.

Figure 10 shows the currents calculated for the condition of Fig. 9. The currents illustrated on the top are those computed under the condition in which only winds are considered; the radiation stress terms were omitted in the momentum equation and τ_s was estimated by using Eq. (7). The currents computed with radiation stress terms are shown in the middle of Fig. 10. When only winds were considered, northeastern currents were developed during the whole period at all the points. When radiation stresses were included, the reversal of the currents was simulated at h = 8.8 m. However, the direction of the currents at h = 15.4 m and 20.0 m was unchanged. Since the significant wave height during this period was 4 m at most, longshore currents would not be developed in the offshore region deeper than 15 m. The reversal of the currents observed after February 1 is therefore considered to be due to the effect of breaking of surface waves. Although the importance of wave breaking in the momentum transfer from the wave motion to the mean motion has been pointed out (Melville and Rapp, 1985; Melsom, 1996), quantitative description is yet to be developed. In the present study, the effect of the surface wave breaking on the development of the currents was incorporated in a rough approach by considering an additional surface stress in the direction of wave propagation. Since stronger momentum transfer will take place

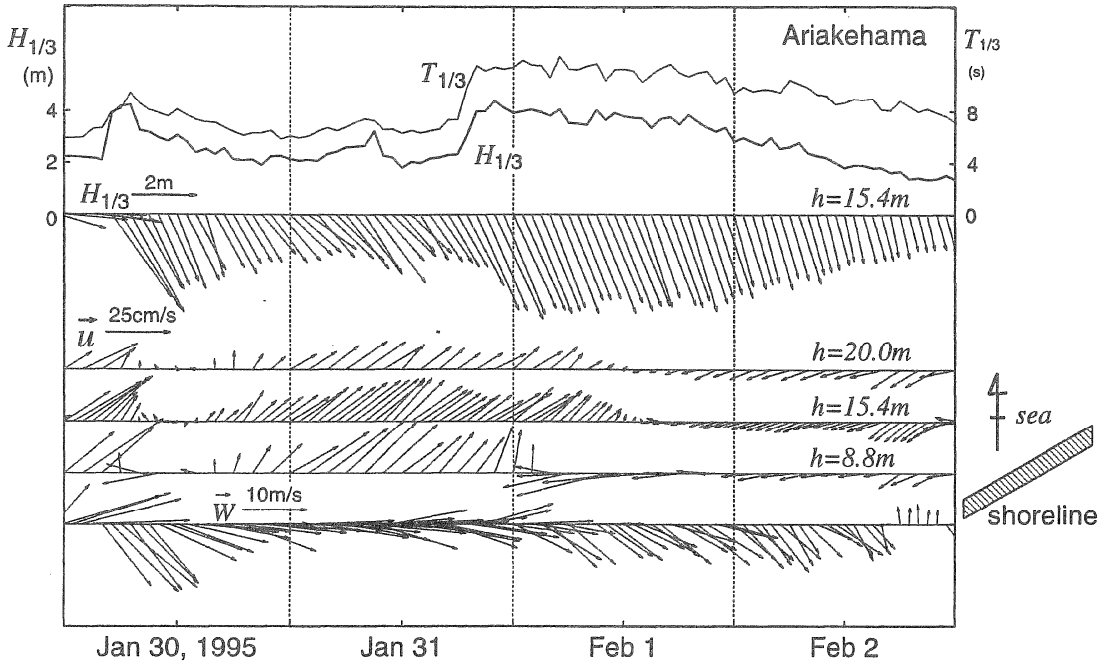

Fig. 9 Distribution of currents at Niigata coast.

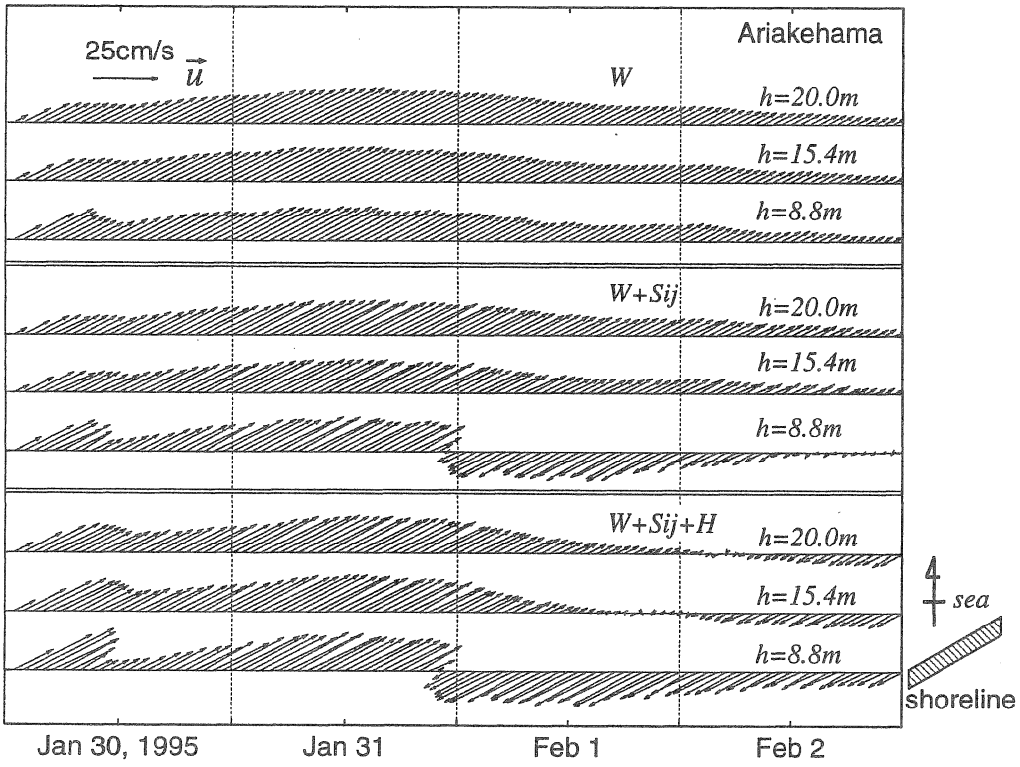

Fig. 10 Distribution of currents computed for Niigata coast.

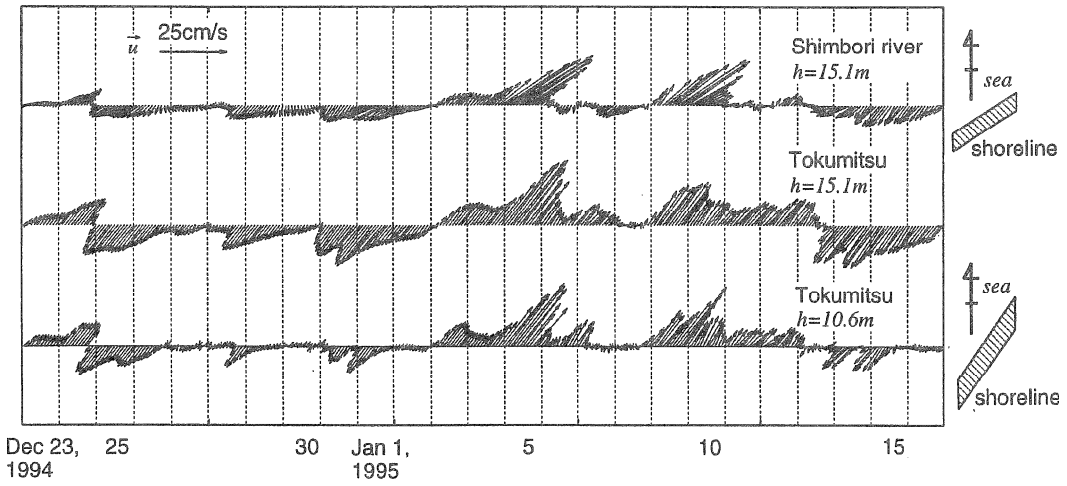

Fig. 11 Temporal variation of currents computed for Ishikawa coast.

under larger waves, the dimensional argument leads to the following equation:

$$\vec{\tau}_s = \rho_a C_a \vec{W}|\vec{W}| + \rho_w C_w g H_{1/3} \frac{\vec{k}}{|\vec{k}|} \tag{10}$$

where $\vec{k}$ is the wavenumber vector and C_w is a non-dimensional coefficient whose value was evaluated at $C_w = 1.0 \times 10^{-5}$ on the basis of the comparison of simulated currents with field data. The currents simulated by using Eq. (10) were illustrated on the bottom of Fig. 10 where the reversal of the currents after February 1 were successfully simulated even in the offshore region. It is also noticed that the observed currents at $h = 8.8$ m were directed slightly offshore owing to the effects of undertow.

3.3 Effect of Coastal Boundary

Figure 5 demonstrated that the currents observed at Shimbori river-mouth were relatively weak compared with those observed at Tokumitsu. Since the Shimbori river-mouth is located in an area sheltered by Cape Kasa, a partial reason for the weak currents might be in the geometry of the coastline. Effects of coastline geometry on the development of currents were examined by a numerical model, in which Cape Kasa and breakwater of Kanazawa Port was modeled. The computation domain was a rectangle with 100 km in the alongshore direction and 30 km in the cross-shore direction. On otherwise uniform 1/100 sloping bottom, Cape Kasa was modeled as a topography protruding seaward in a triangular region 10 km in the alongshore direction and 2 km in the offshore direction (scc Fig. 2). The presence of the breakwater of Kanazawa port was modeled in a crude manner as a straight jetty extending to 1.5 km offshore. The wind field was assumed to be uniform in the whole domain and wind velocities observed at Tokumitsu were used as the input to the model.

Figure 11 shows computed currents at the measuring points on Ishikawa coast. It is noticed that the currents at Shimbori 15.1 m was smaller than those at Tokumitsu, indicating that the magnitude of the wind-driven currents was influenced by coastal topography. However, the magnitude of the computed currents was still larger than

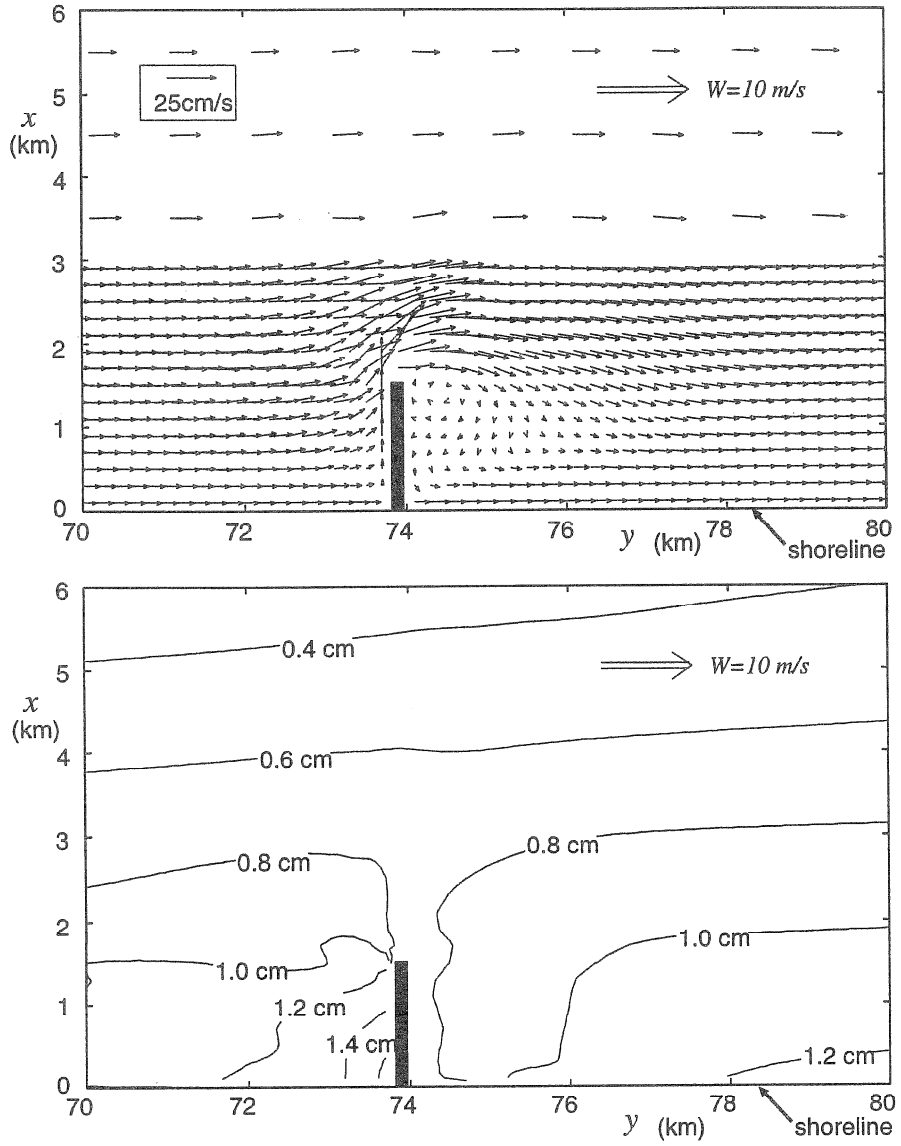

Fig. 12 Currents and mean water level computed around a long jetty.

the measurements, indicating that other factors such as the three-dimensional local topography and the non-uniformness in the wind field must be incorporated in the model to elucidate the weak currents observed at Shimbori 15.1 m.

Figure 12 shows the currents and the mean water level change computed for the condition of alongshore wind of 10 m/s blowing over a straight jetty on a 1/100 sloping beach. The figure illustrates the equilibrium state after the wind continued to blow for 2 days. The Coriolis force was included in the computation but the effects of waves on currents were not included. The eddy viscosity was set at 1 m^2/s. Together with the overall windward currents, strong offshore-directed currents and the rise in mean water level were developed on the upstream side of the jetty. On the downstream side of the jetty, a large eddy was developed in a region extended about two times of the

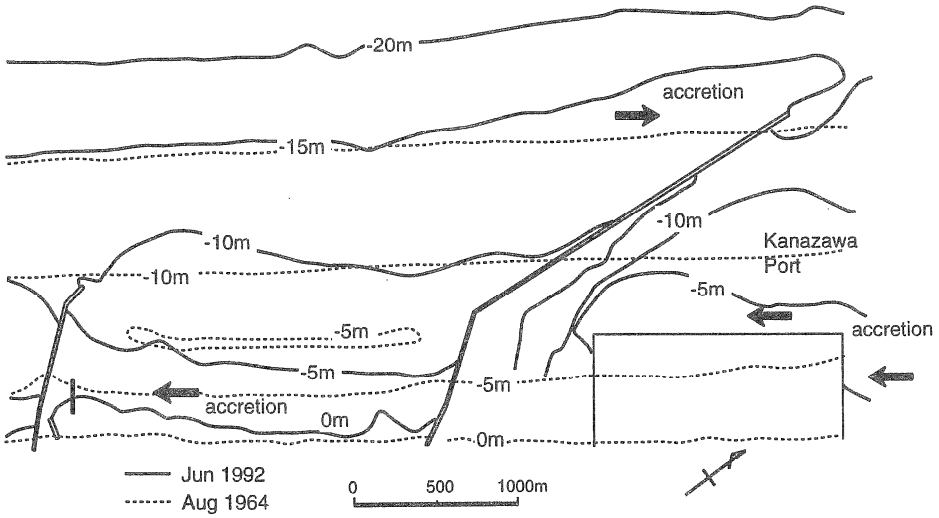

Fig. 13 Bottom topograhy change in the southern area of Kanazawa port.

jetty length. It is therefore confirmed in numerical experiments that the large-scale currents are influenced by coastal topography and large-scale structures.

Figure 13 illustrates the change in bottom topography observed around Kanazawa Port. Wave records indicated that the direction of the net longshore transport on this coast was from the north to the south. The shoreline deformation shown in Fig. 13 also confirms that the dominant direction of longshore transport in surf zone is from the north to the south. However, in the offshore region, significant accretion was observed on the south side of the breakwater, which is considered to be due to the large-scale currents described in the present study. Analysis of the bottom sounding data demonstrated that the average rate of the accretion on the southern side of the breakwater was 1.4×10^5 m^3/yr. A quantitative explanation on the rate of the accretion must be made in the future study on the basis of the annual data of winds, waves and currents.

IV. CONCLUSIONS

Field data of waves, currents, winds and bed elevation change obtained at Ishikawa and Niigata coasts facing the Japan Sea were analyzed and compared with numerical simulation. Major conclusions are as follows: (1) Large-scale alongshore currents were developed in the offshore region after the passage of a low-pressure system. (2) Numerical simulation confirmed that the currents were driven by the wind stress and the momentum transfer due to surface wave breaking. (3) The currents interacted with nearshore currents developed in surf zone. (4) The bed in the offshore region was observed to be scoured significantly by steep waves at the early stage of a storm.

It was also suggested that the large-scale currents could be responsible for large-scale evolution of coastal topography. Further investigation is needed to estimate the effect quantitatively.

ACKNOWLEDGEMENTS

The author wishes to express his sincere thanks to the Shinanogawa-karyu office and the Kanazawa office of Hokuriku Regional Construction Bureau, Ministry of Construction, for providing valuable data.

REFERENCES

Goda, Y. (1975): Irregular wave deformation in the surf zone, Coastal Eng. in Japan, Vol. 18, pp. 13–26.

Goda, Y. and N. Watanabe (1991): A longshore current formula for random breaking waves, Coastal Eng. in Japan, Vol. 34, No. 2, pp. 159–175.

Honda, T. and H. Mitsuyasu (1980): Laboratory study on the effects of wind on sea surface, Proc. 27th Japanese Conf. on Coastal Eng., pp. 90 93 (in Japanese).

Longuet-Higgins, M. S. (1970): Longshore currents generated by obliquely incident sea waves, J. Geophys. Res., Vol. 75, pp. 6778–6801.

Melsom, A. (1996): Effects of wave breaking on the surface drift, J. Geophys. Res., Vol. 101, No. C5, pp. 12071–12078.

Melville, W. K. and R. J. Rapp (1985): Momentum flux in breaking waves, Nature, Vol. 317, No. 10, pp. 514–516.

Niedroda, A. W. and D. J. P. Swift (1991): Shoreface processes, in Handbook of Coastal and Ocean Engineering, Gulf Publishing Company, pp. 735–770.

Sato, S. (1995): Characteristics of currents induced by low pressures in the Japan Sea, Coastal Eng. in Japan, Vol. 38, No. 1, pp. 5–18.

(Received Sep. 17, 1996; Revised Nov. 1, 1996)